Environmental and Sustainability Indicators 25 (2025) 100570

Contents lists available at ScienceDirect

Environmental and Sustainability Indicators

journal homepage: www.sciencedirect.com/journal/environmental-and-sustainability-indicators

Geohazard mapping and mitigations along the road corridor Gasera–Indeto, Southeast Ethiopia

Chalachew Tesfa

Debre Markos Technology Institute, Debre Markos University, Ethiopia

ARTICLE INFO

Keywords:
Landslides
LSM
AHP
FR
GIS
And Southeast
Ethiopia

ABSTRACT

The study area is one of the biggest gorges in southeast Ethiopia formed by the Wabe Shebelle river. The road was constructed to connect Gasera to Indeto. The study aimed to map and gives some mitigation strategies for geohazards along the road corridor in Southeast Ethiopia using a GIS with AHP & FR technique within the 3 km buffer zones along the road corridor. The study included field investigations and inventorying, characterization of geological situations, assessments of the hydrogeological conditions, and identification of slope instability variables. A GIS technique was used to map an LSM with the combination of two models (AHP and FR). The study used eight factors: slope, aspect, lithology, rainfall, altitude, road proximity, river proximity, and land use/cover. The results of the study revealed that LSZ maps performed using FR and AHP were 64.5 % and 69 % and-the inventory shows high and very high LSZ respectively. Rockfalls, debris/earth slides, and rockslides are commonly observed landslides in the area. Based on the analysis lithology (basaltic and limestone formations) showed the highest contributions for landslide in the area. Slope and aspects show the most frequent landslide hazards in >40, 30–40°, and east, and northeast respectively. Generally, the study found that lithology, slope, and aspect were the main factors contributing to slope instability in the study area. The produced landslide susceptibility map is very important for urban planners, agricultural studies, environmentalists, and future landslide hazardous prevention and mitigation strategies.

1. Introduction

Landslides are a common problem across the world and it is also a serious problem here in Ethiopia. Many researchers (Woldearegay, 2013; Tesfa and Woldearegay, 2021; Hamza and Raghuvanshi, 2017; Asmare and Tesfa, 2022; Tesfa, 2022; Gnyawali et al., 2015) have done different research on landslides and related studies in different parts of the world including in Ethiopia. According to varieties of engineering activities such as highways, railways, and dams for transportation, power production, and water supply, industrial and urban development require the excavation of massive rock formations (Wyllie and Mah, 2004; Zhu et al., 2022). The localities exploit ragged areas for habitation, and farming, as well as for settlements due to an increase in population and a scarcity of land resources in Ethiopia. These efforts frequently tend to alter stable areas and exacerbate the problem of sliding. The human cost of global warming and deadly landslides with their triggers was discussed (Haque et al., 2019). A landslide is a major natural disaster that has resulted in significant injury and loss of life, as well as damage to property and infrastructure all over the world. The Ethiopian Highlands are frequently subjected to a variety of geohazards that cause instant harm to nearby people and property and undergo some processes that change their condition from stable to unstable (Tesfa and Woldearegay, 2021; Hewitt, 2016; Asmare et al., 2023). This is essentially due to a decrease in the shear strength of the slope materials. According to (Tesfa, 2022), in most cases, the instability of an area is due to the fragile nature of the geological materials and heavy rainfall associated with intensive stream discharges. Recent flooding and landslide events in an urban context around the world have further highlighted the need for assessing geo-environmental hazards and risks in urban planning and management. In Ethiopia, landslide-generated hazards are becoming serious concerns for the general public and the planners and decision-makers at various levels of the government (Woldearegay, 2013). However, so far, little effort has been made to reduce losses from such hazards. Naturally occurring geohazards are complex natural occurrences that take place across the nation at predictable times and under certain circumstances (Ahmad and Khan, 2023; Mishra et al., 2024). Particularly in recent years, there has been progress in a better understanding of landslide initiation and techniques for

E-mail addresses: chalachew_tesfa@dmu.edu.et, chalachewtesfa@gmail.com.

https://doi.org/10.1016/j.indic.2024.100570
Received 25 August 2024; Received in revised form 22 December 2024; Accepted 24 December 2024
Available online 26 December 2024
2665-9727/© 2024 The Author. Published by Elsevier Inc. This is an open access article under the CC BY-NC license (http://creativecommons.org/licenses/by-nc/4.0/).

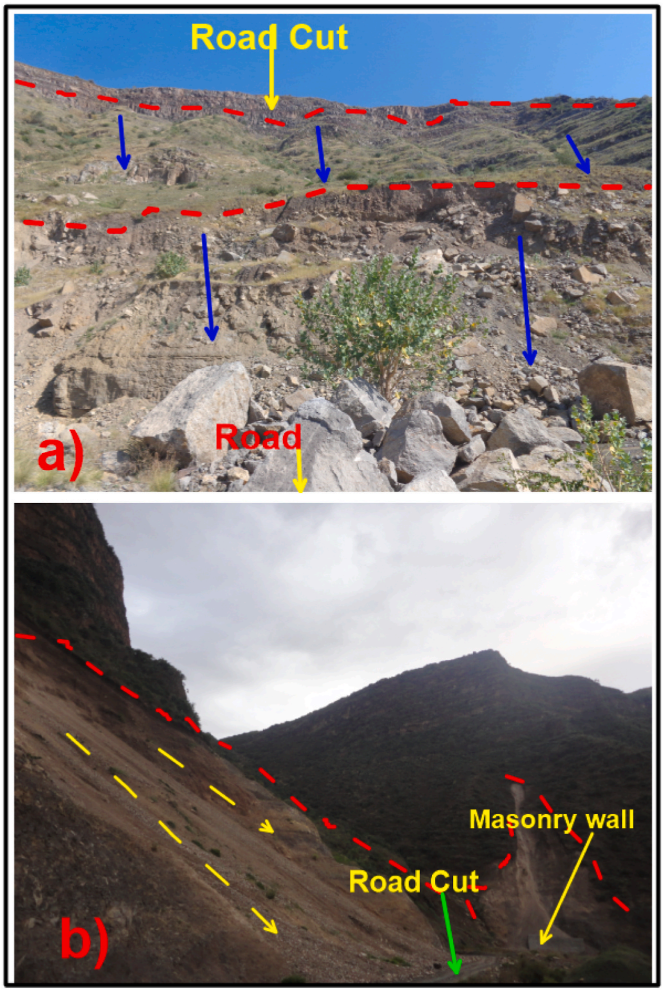

Fig. 1. Some of the slope failures: (a) mass movement and (b) debris sliding.

assessing, predicting, and mitigating slope instability hazards (Korup and Stolle, 2014; Choudhury et al., 2024). Despite such advancements, landslides continue to prevail in both developed and developing countries, with larger casualties in developing nations but severe economic losses in the industrialized world. The study area is found in the Gasera, Wabe Shebelle Gorge in the Eastern of the Ethiopian rifting system and the Southeastern plateau of Ethiopia. The flow of the Wabe Shebelle river from the upper part of the Melka Wakena Hydro-Electric Dam site drains in the Indian Ocean after traveling 1130 km in Ethiopia. Wabe Shebelle river is one of the largest rivers in Ethiopia that drains across the country towards the Indian ocean. The river has a great contribution to the occurrence of border country Mogadishu, the capital of Somalia, like another river great Abbay to Sudan, Egypt and others to the downstream.

The increasing demand for road networks has led to an increase in road construction in Ethiopia. On the Gasera–Indeto road, along Wabe Gorge, landslides and slope instabilities along the road sections of the newly constructed gravel road are rock falls, rock slides, debris, and earth materials are the common land instability problems observed in the area (Fig. 1 a & b). People living in the Gasera Gorge are severely impacted by road cuts, debris, and/or earth slides caused by road-building operations in this region as a result of the road-cut exposures. The road from Gasera to Indeto is constructed across the wabe shebelle gorge which has a very difficult topography and a very hot temperature. People in the area are agriculturalists they produce different types of fruits and agricultural products. These largely produced products need to be transported to the Gasera area in most cases they transported them traditionally so for this purpose the road was constructed.

Generally, the sloping materials affect the agricultural fields, natural environments, and streams that the localities use for irrigation, and the road is covered by slope materials and cuttings from the road excavations and the rock falls (Fig. 1 a & b). As a result, this research was to produce a hazard zone map of the region, designate the different important and unstable hazard locations in terms of risks, and provide potential solutions to the problems as well as consecutive landslides in the area. The AHP (Analytical Hierarchy Process) method works by conducting a ratio scale from a paired comparison matrix which relies on the expert's judgment and prioritizations (Desalegn et al., 2022). To determine the priority of landslide causative factors and convert the oral descriptions to quantitative values (Dastranj and Noor, 2021). According to FR (Frequency Ratio), the parameters and variables, the integration with inventory, and the weight classes were established using the frequency ratio (Equation (4)). At the last, a relationship between landslide factoring variables and the inventory assessed in Arc GIS with the integration of AHP and FR values to generate landslide susceptibility and hazard zonation maps (Wang and Li, 2017; Klai et al., 2017). So, the study aims to understand and identify the possible causes of landslides in this area and to recommend possible mitigation measures to minimize the past landslide-affected areas as well as to delineate the future

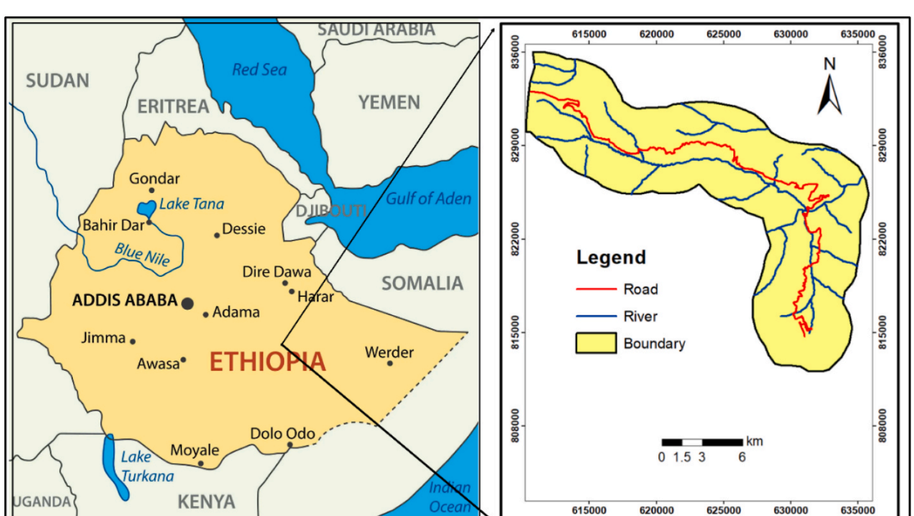

Fig. 2. Location map of the stud area.

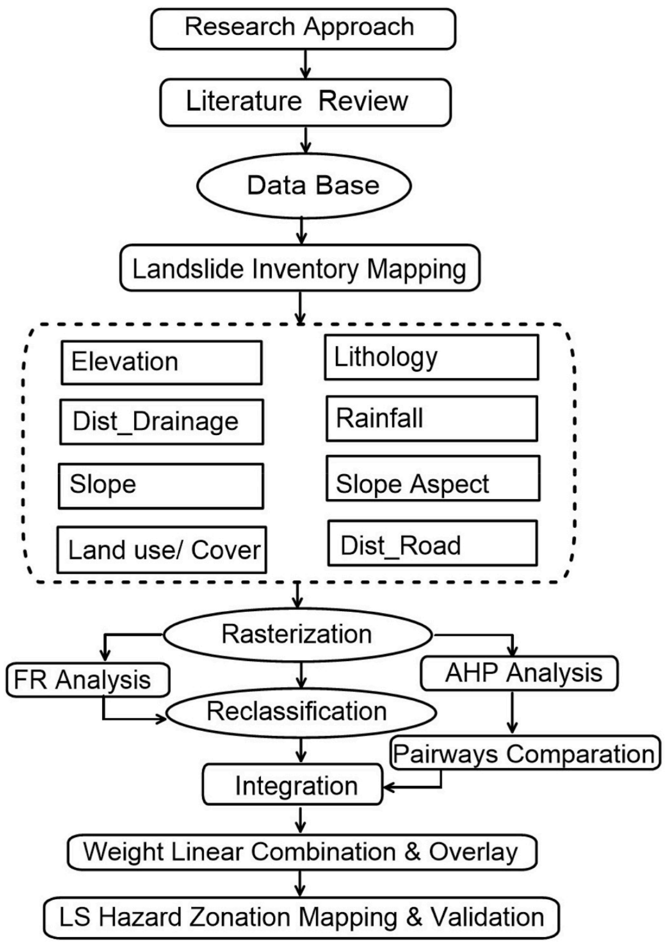

Fig. 3. Flow charts followed by the approach.

landslide susceptible zones in the area. In addition to this, the research is planned to assess and study the geology, hydrogeology, and geological structures of the study area and their influence on the stability of the area as well as recommend some selected mitigation measures.

1.1. *Description of the study area*

The study is situated at the Wabe Shebelle river gorge. Geographically the study area is bounded from North to South by latitude 40◦ 1′ 25.7" to 40◦ 14′ 30.7" and from West to East by longitude 7◦ 21′ 14" to 7◦ 34′ 45.9" (Fig. 2). The study area is accessible by an asphalt road that connects Addis Ababa (capital city of Ethiopia), to Nazareth– Asela– Dodola– Robe (412 km asphalt road) and then Gasera 60 km gravel road from Robe.

2. Methodology and research approaches

There are different methods of landslide analysis among different methods or approaches, two methods (AHP and FR) approach are selected for this study. The two models are selected for this study due to their strength and large acceptance by different researchers and scholars worldwide. To evaluate landslide hazards, a variety of methods are followed (Fig. 3). The study's secondary data came from governmental and non-governmental organizations, journals, the internet, and other sources, while the main data came from field surveys/observations, satellite pictures, local DEMs, Google Earth imagery, and a topographical map of the study area served as the primary sources of information for this study.

The slope, elevation, and aspect were formed using the DEM data. Another set of data used in this study was the average annual rainfall of metrological stations, obtained from the National Meteorological Agency of Ethiopia. The main road and river were digitized from the topographical map of Ethiopia. The other sets of landslide data were digitized from the study area using Google Earth imagery and field surveys. All the data layers have been constructed and combined in the ArcGIS 10.4 tool. The ArcGIS tool was applied throughout the whole process in this study.

A) AHP Method

The AHP was a multicriteria managerial process based on the decisions of the professionals (Dos Santos et al., 2019). The AHP provides a means of decomposing the problem into a hierarchy of sub-problems that can more easily be comprehended and subjectively evaluated. AHP can be explained in the following steps.

Step 1: Develop a hierarchy of goals, criteria, sub-criteria, and alternatives. According to (Saaty, 2008), an effective technique to organize the hierarchy is to work down as far as feasible from the objective and then move up from the alternatives until the levels of the two processes are linked in such a manner that comparisons are conceivable.
Step 2: Collect data from the experts and/or decision-makers equivalent to the hierarchic structure with pair-wise judgment alternatives.
Step 3: Organizing the pair-wise decision-making data into a square matrix of the diagonal is 1.
Step 4: Check the eigenvalue and the corresponding normalized eigenvectors are the comparison matrix to give the relative importance of the various criteria being compared.
Step 5: Evaluate the consistency matrix order *n.* If this consistency index fails, it is until the required level answers the comparisons. The consistency index, CI, is calculated as:

$$CI = (\lambda \max - n)/(n - 1) \tag{1}$$

Where: λ max is the max eigenvalue in the matrix. n is the total number of factors in the matrix. CI the compared random matrix, RI. The ratio derived, CI/RI, is termed the consistency ratio, CR. (Saaty, 2008) suggests the value of CR should be less than 0.1.

$$CR = CI/RI \tag{2}$$

Where: RI is the average consistency index depending on the order of the matrix given by (Saaty, 2008).

Step 6: The rating of each alternative is multiplied by the weights of the sub-criteria and aggregated to get local ratings concerning each criterion. The local ratings are then multiplied by the weights of the criteria and aggregated to get global ratings. The AHP produces weight values for each alternative based on the judged importance of one alternative over another concerning a common criterion. LSI can be calculated by using Equation (3) Given by (Voogd, 1988).

$$LSI = \sum_{i=1}^{n} (Wj*Wij) \tag{3}$$

Where: LSI is the landslide susceptibility index, *Wj* is the weight value of parameter *j*, *wij* is the rating value or weight value of class *i* in parameter *j*, and *n* is the total number of factors (Table 4), n is the number of factors.

B) Frequency Ratio methods

The FR is implemented to establish spatial variations of landslide location and parameters (Lee and Talib, 2005; Anbalagan et al., 2015).

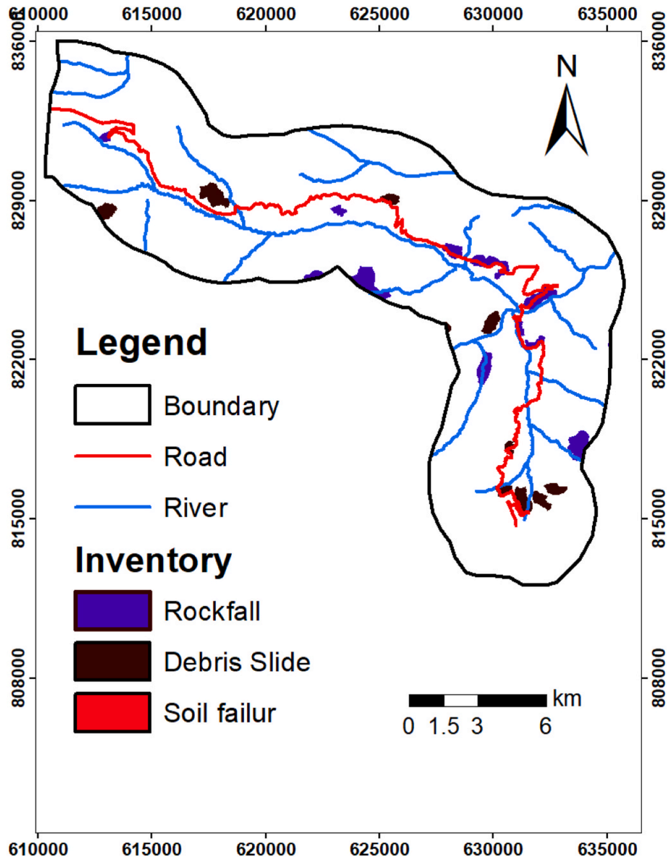

Fig. 4. Landslide inventory mapping.

Fig. 5. Figures showing Rock falls a) and Debris slides b) that hinder and/or close the road.

This relationship is expressed quantitatively by the frequency ratio of landslides in each class of each causative factor and the area of the respective class compared to the total of the studied area territory. According to (Lee and Talib, 2005), a higher ratio shows stronger correlations between the observed and causative parameters of landslide (Asmare, 2022; Tesfa and Sewnet, 2024). The information on different layers of landslide factor maps was prepared and classified. These layer maps will be combined with the information on landslide distribution and the landslide polygon maps determined in each class of parameters.

$$FR = \frac{\text{\% of occurrence in each class}}{\text{\% of the area in a related class}} \quad (4)$$

$$LSI = \sum_{i=1}^{n} FR \quad (5)$$

Where: FR is the ratio value; n is the total parameters.

3. Results

3.1. Landslide inventory

The inventory mapping of landslides in the area was done using a variety of techniques such as field surveys, interpretation of satellite images, interpretation of aerial photography, Google Earth imaging, and literature reviewing from past historical landslide records, technical and government reports, expert interviews, as well as scientific reports. The concentrations of landslides are more hazardous in road cut exposures. In the study area, there are also rockfalls along the road cut, and several rockfalls were observed in some parts of the area on the cliff sides (Fig. 4). The rock falls mostly observed in the area are limestone embolisms and basalts. Rock falls are mostly observed as the road cut exposure along the road corridor is formed due to blasting and unstable cut slope angle.

Due to the occurrence of weak zones between the two separate layers of limestone and basalt units, a weak sub-horizontal-horizontal layer dividing two limestone layers, seepage of water into the weathered and cracked layers that are exposed on the surface after the construction of the road.

Orientations of discontinuity and the road: Steep slopes average 70-85° dips making the rock slope disaster for the rock falls observed in Wabe cuts in limestone units. The debris slide direction is perpendicular to the road cut which leads to an unstable slope and that is the reason observed debris slides along the road corridors.

Discontinuity in Beddings: Basically, the marl layers were observed in limestone-shale- marl units this leads to eroding rapidly and simply due to gully or rainwater therefore the superimposing interconnected rock masses misplace their underlining sustenance and lastly drop.

Gully Erosion/debris flow: Surface runoff is accelerated because of excessive rainfall and the sharp hilliness of the area. The severely jointed and fractured boulders begin to separate upward, with the runoff water bringing the blocks and fragments down. Many gullies occur, and smaller rock fragments float in the waterway unsteadily.

Rockfall: Rock falls, at some specific locations along the road corridors rock falls are observed and mostly the geology of the slope area is basaltic rocks and limestone units are highly exposed to/by rock falls relatively. The observed rock falls along the road corridor are caused by blasting activities and the rock falls out of the road corridor are caused by natural phenomena. The size of the rock fall blocks varies from some centimeters to a meter and is sometimes even larger than 1.5m in

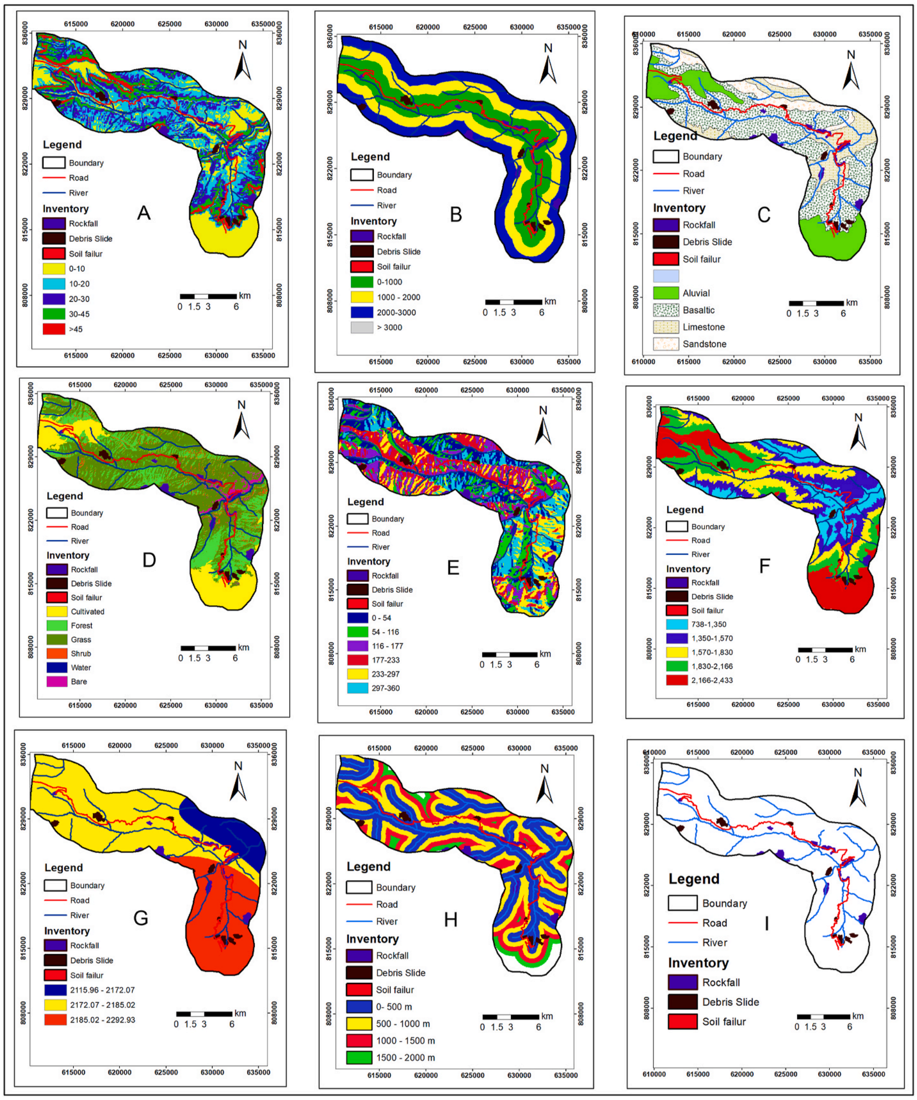

Fig. 6. Causative factor maps of the area A) Slope degree of the area B)Road distance map C) Lithology map D)Land use Land cover map E) Aspect Map F)Altitude Map G) Rainfall Map H) Stream/River distance map and I) Shows the landslide Inventory Mapping.

diameter. It was detected that the weak layer of marl and/or shale unit underlying the limestone units facilitates rapid erosion due to seepage (Soni et al., 2022; Wicki et al., 2022), undermining the adjacent rocks and causing rock failure (Fig. 5 a).

3.2. Causative factors

Comprehensive field study of the slope insatiability areas and selection of the different causative factors that can initiate the landslides of the area. Based on the site condition of slope instability areas, eight (Zhu et al., 2022) influencing factors were selected for further determination and analysis of the degree of initiation and influence. The details of each causative factor are expressed as follows.

Slope Degree: This is the most influencing parameter that contributed to the occurrence of instabilities. It was derived from DEM with a cell size of 30 by 30 m and was classified into five different slope classes based on the degree of the class area 1 (0–10), class 2 (Hewitt, 2016; Asmare et al., 2023; Ahmad and Khan, 2023; Mishra et al., 2024; Korup and Stolle, 2014; Choudhury et al., 2024; Desalegn et al., 2022; Dastranj and Noor, 2021; Wang and Li, 2017; Klai et al., 2017; Dos Santos et al., 2019), class 3 (Dos Santos et al., 2019; Saaty, 2008; Voogd, 1988; Lee and Talib, 2005; Anbalagan et al., 2015; Asmare, 2022; Tesfa and Sewnet, 2024; Soni et al., 2022; Wicki et al., 2022; Lin et al., 2022; Das et al., 2022), class 4 (30–45) and class 5(>45) (Fig. 6A). The occurrences of landslides in this class based on the inventory are the target to study and show in the Table:

Road Proximity: the Gasera - Indeto -road alignment is also considered the contributing factor to the instability of the area. Therefore, road distance maps were prepared from analyst tools in the GIS environment. The frequent failures are observed on the sides of the road cut exposures consecutively this means that the road cut may be unstable or the road vibrations by vehicles induced landslides in the area (Fig. 6 B).

Lithology: Lithology was covered by four different units. These are fluvial deposits, Basalts, limestone, and sandstone (Fig. 6 C). The occurrence of failures is mostly observed in the limestone and sandstone units.

Land use/Land cover: this map was prepared from the data of the Geomatics Center of China with a subclass of forest land, grassland, shrubland, water bodies, cultivated land, and bare lands. Finally, it was converted into a shape file and exported to Arc GIS software (Fig. 6 D).

Slope Aspect: The area's slope face map is prepared and classified. The occurrence of landslides in this component may be controlled by this factor such as exposure to sunshine, drying winds, rainfall, and

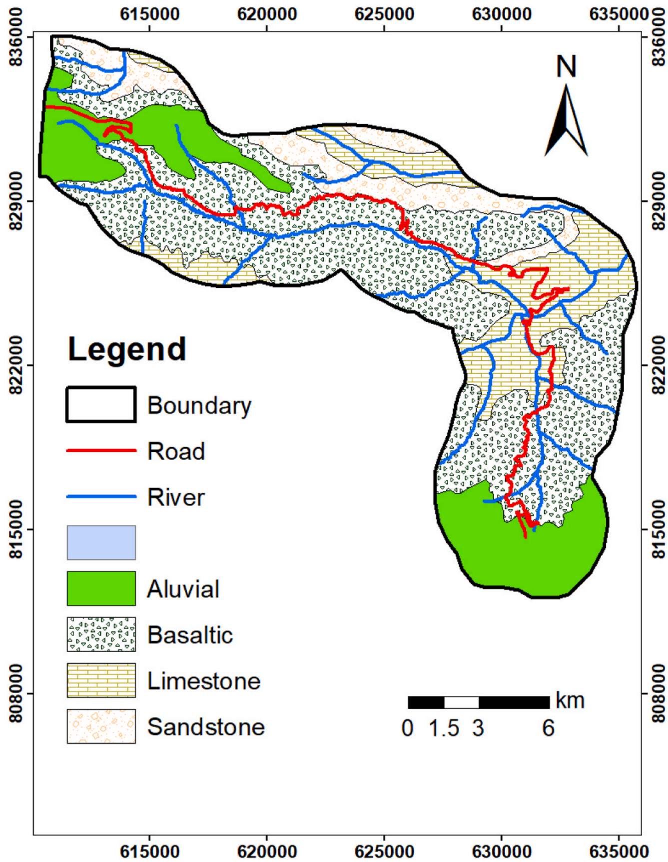

Fig. 7. Shows a Geological map of the study area.

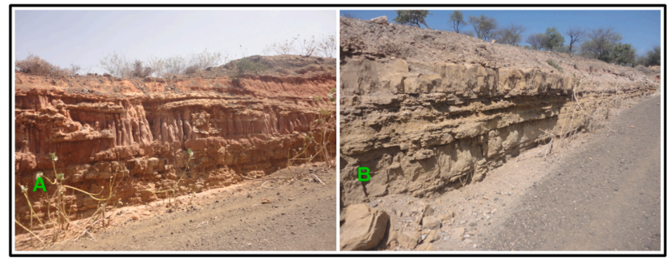

Fig. 8. Limestone marl intercalations observed on the road cut side.

Fig. 9. Road cut Exposure of Aphanitic basalt intercalation with scoria around Gasera at the entrance of the gorge's southern part.

discontinuities. Landslides mostly occurred in the East, Southeast, Southwest, and West aspect subclass areas (Fig. 6 E) and (Table. 3&5).

Altitude: Using DEM 30m-by-30m digital elevation model by using the Arc GIS 10.4 and depending on the topography of the area classified into (738–1350), (1350–1570), (1570–1830), (1830–2166), and (2166–2433). The lowest and highest points are 738 and 2433 m respectively above sea level (Fig. 6 F).

Rainfall: rainfall is the one influence for the initiation of failure (Lin et al., 2022; Das et al., 2022). For this study, the average precipitation data are collected at four existing rain gauge recording sites of the past years (2000–2016). The recording places are situated inside and outside of the study area Northeast (Sedika), southeast (Jara), West (Agarfa), and South (Gasera), and the average yearly precipitation of these four stations is recorded to be 2264.98 mm, 1187.97 mm, 2236.74 mm, and 2292.93 mm respectively (Fig. 6 G).

River Proximity: River distance map shows the occurrence of surface, and sub-surface water in the area, and similarly, that can show the weak zones and shear zones of the area. In the area, Wabe Shebelle, Robe, and other tributaries incised the geological units. Stream distributions are obtained from DEM and from a topographical map of the study area that was edited by using Arc GIS 10.4 and a river distance map produced with a 250m buffer zone in the analyst tools found in the GIS windows (Fig. 6 H). Field observations show that there are gully erosions in some areas and from the drainage patterns at some places river erosions and that is observed at the bank of the river sediment deposits.

3.3. *Geological setting of the study area*

The Geological setting of the area shows Ethiopian geology exposed due to the Wabe Shebelle river cut exposure. In the study area except for the basement rocks the sedimentary and basaltic rocks are observed (Fig. 7). Based on field observations and geological formations the lithology of the area is described as follows.

3.3.1. *Sandstone and siltstone intercalations*

The sandstone and siltstone units were observed as road cuts and valley cuts of the gorge at the northeastern portion of the area. This unit is thin, variegated sandstone overlain by medium to thick-bedded sandstone with an average thickness of 0.5–1m (Fig. 8 A). Based on the field survey, the orientation of the sandstone stratum is to the southeast (Fig. 8 A). In the top half of this region, sedimentary formations such as bedding planes and laminations are observed.

3.3.2. *Limestone*

The limestone unit shows yellowish-light brown varying colors and thinly to medium bedded, planar, laminated, horizontal, continuous bed, fine to medium grain size, and at some places observed distributed

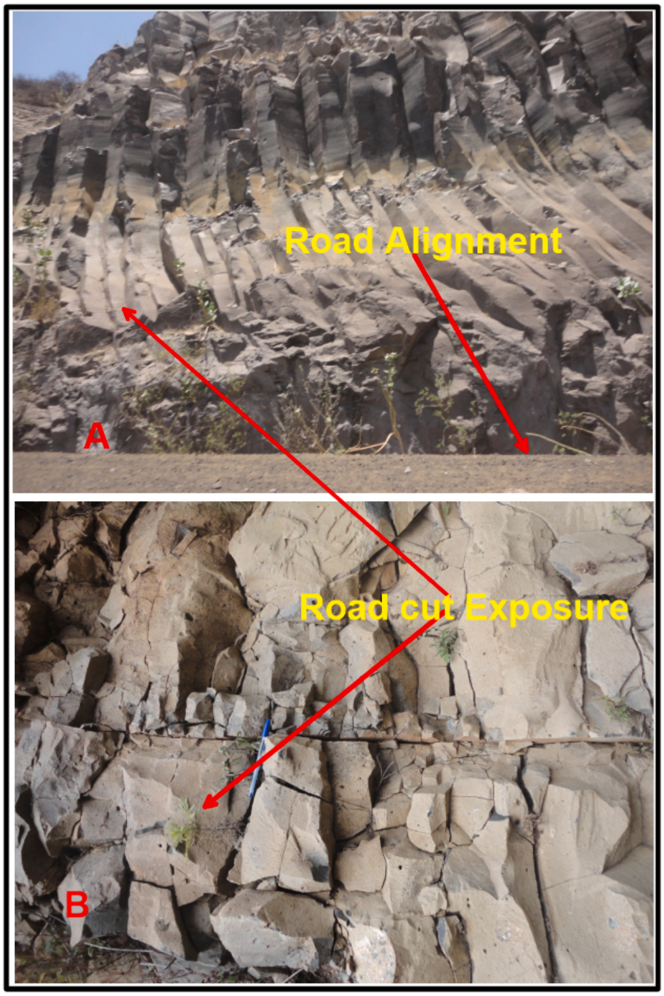

Fig. 10. Geological structures observed during field survey.

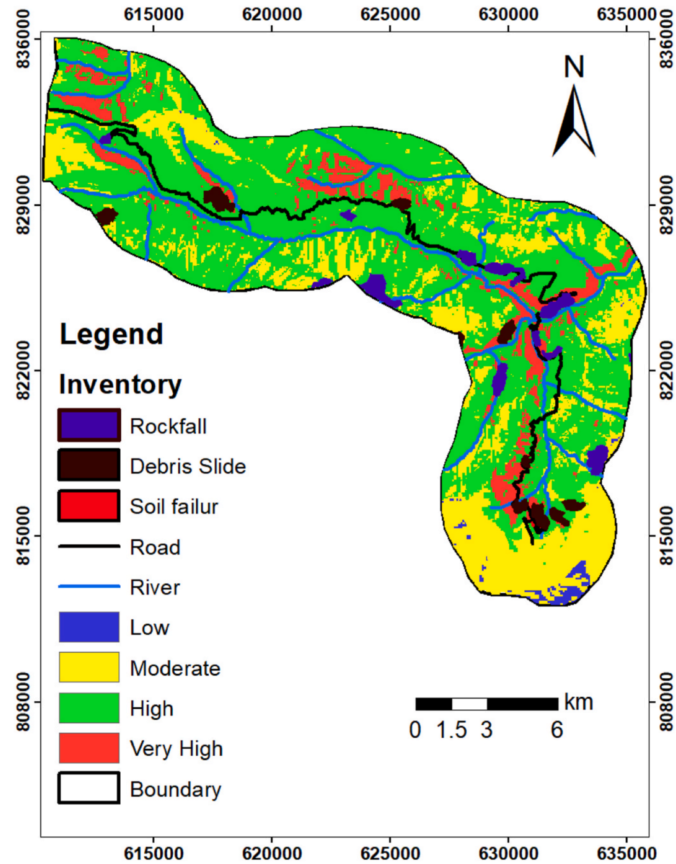

Fig. 11. Landslide susceptibility Index map produced by the AHP model.

patterns of bedding strata (Fig. 8 B). The thickness differs from place to place in this rock unit as can have been observed from the Wabe Shebelle river cut; they noted an extremely exposed thickness was 450m. The beds are showing varying thicknesses ranging from less than 0.5 m to 1m alternating (Fig. 8 B).

3.3.3. Basaltic rocks

This lithology is dominant in the area and covers a large part compared to the sedimentary units in the study area (Fig. 7). These units are further classified according to composition, texture, Lithological setting, and structural formations as aphanitic basalt with intercalations scoria, vesiculated basalt, and dolerite intrusions.

Aphanitic basalt intercalated with Scoria: this unit was exposed as hillside, river cut, and road cut exposure with a thickness range from 10 to 25 m. It shows the high weathering rate and fractured in the exposed area, especially it is visible at the road cut exposures. The top part of this unit is covered by weathered residual soil at the top and scoriaceous vesicular basalt with varying degrees of weathering of around 6m thickness (Fig. 9).

Aphanitic basalt with intercalation of vesicular basalt: This unit has occurred in the central part of and occupies a significant portion of the study area. Columnar jointed and vertically stratified basalts are frequent, and some are extensively worn and fractured. They are aphanitic in texture, with a new dark grey tint and an aged light grey.

Dolerite intrusions: are observed in the central part and exposed as cliff side and cliff top. This unit has a grey fresh color as well as a light grey of an altered color. The depth ranges from 5 to 10m and at some locations it shows spherical weathering with a 5 cm - 1m block size.

Quaternary Deposits: This includes alluvial residual soils and colluvial deposits and the alluvial originated from the basaltic rock units and underline highly weathered basalt. This unit is a weathering product of the basaltic, scoria, and some other rocks from the Bale Mountain areas and other highland areas. Its thickness ranges from 20 to 30m observed in the road cut and valley at the entrance of Gasera gorge and Indeto southern and north parts. This portion is a densely populated region; the local people use this area for settlements and their agricultural activities because of the percolation and fertility of the soil. In some parts of the gorge and Wabe river also these materials are deposited and the Weredubey peoples who live around the Wabe river use them for agricultural activities and irrigation purposes.

3.3.4. Geological structures

The geological structures that are mostly observed are faulting, beddings, lineaments, dykes, and joints are common during field observation.

Bedding and Stratification: These structural measurements are commonly observed in sedimentary units. Mostly the beds show horizontal stratifications between the limestone and marl shale intercalations on the limestone rock unit. These structures are the primary structures that are formed during the sediment deposition of sedimentary units. These bedding and planes clearly show the surfaces that separate one stratum from another in the sedimentary rock units, especially in limestone. This bedding structure shows horizontally aligned structures trending N-S (Fig. 8B).

Joint: This structural feature is commonly observed on aphanitic basalt and other units with varying geometry and orientation. It shows vertical to sub-vertical trending with an orientation of NE45-75SW (Fig. 10A).

Dikes: This geological structure is a basaltic dyke observed in the

Table: 1
Pair-wise comparison matrix for calculating weights (first step).

Weight Decision Matrix	[1]	[2]	[3]	[4]	[5]	[6]	[7]	[8]	Weights
[1] Rainfall	1.00	2.00	2.00	4.00	5.00	6.00	7.00	8.00	0.31
[2] Slope	0.50	1.00	2.00	3.00	4.00	5.00	6.00	7.00	0.23
[3] Lithology	0.50	0.50	1.00	2.00	3.00	4.00	5.00	6.00	0.17
[4] Altitude	0.25	0.33	0.50	1.00	2.00	3.00	4.00	5.00	0.11
[5] Road Proximity	0.20	0.25	0.33	0.50	1.00	2.00	3.00	4.00	0.07
[6] LU/LC	0.17	0.20	0.25	0.33	0.50	1.00	2.00	3.00	0.05
[7] River Proximity	0.14	0.17	0.20	0.25	0.33	0.50	1.00	2.00	0.03
[8] Aspect	0.13	0.14	0.17	0.20	0.25	0.33	0.50	1.00	0.02
Total	2.88	4.59	6.45	11.28	16.08	21.83	28.50	36.00	1.00

Table: 2
Arithmetic Mean for weights parameter calculation in AHP method (second step).

Weight Decision Matrix	[1]	[2]	[3]	[4]	[5]	[6]	[7]	[8]	Reciprocals	λ_{max}
[1] Rainfall	0.35	0.44	0.31	0.35	0.31	0.27	0.25	0.22	2.885	0.902
[2] Slope	0.17	0.22	0.31	0.27	0.25	0.23	0.21	0.19	4.593	1.062
[3] Lithology	0.17	0.11	0.16	0.18	0.19	0.18	0.18	0.17	6.450	1.069
[4] Altitude	0.09	0.07	0.08	0.09	0.12	0.14	0.14	0.14	11.283	1.222
[5] Road Proximity	0.07	0.05	0.05	0.04	0.06	0.09	0.11	0.11	16.083	1.186
[6] LU/LC	0.06	0.04	0.04	0.03	0.03	0.05	0.07	0.08	21.833	1.092
[7] River Proximity	0.05	0.04	0.03	0.02	0.02	0.02	0.04	0.06	28.500	0.973
[8] Aspect	0.04	0.03	0.03	0.02	0.02	0.02	0.02	0.03	36.000	0.874

basaltic unit and shows an orientation of N10° W. It is exposed in the northern part as hillside and road cut exposure.

Fault: Faults are geological structures that can affect and disturb the normal natural appearance of lithological units and many types of manmade structures like highways, building structures, hydraulic structures, and mining operations. In the study area, there are some normal faults are observed. Generally, the faults exposed on basaltic and limestone rocks show N – E, to S – W trending.

3.4. Landslide susceptibility mapping (LSM) using AHP method

Landslide susceptibility mapping by using AHP (Fig. 11) was prepared based on the calculated ratio value of CR obtained from the ratio value CI matrix's consistency index, according to equation (2) the random index RI, which is the average consistency index. According to (Millet and Saaty, 2000) the acceptable range of CR varies based on the size of the matrix i.e., 0.05 for 3by3, 0.08 for 4by4, and 0.1 for all more than $n > 5$ matrices. The principal eigenvalue is obtained from the products between each component of the eigenvector and the sum of columns from the reciprocal matrix (Table 1).

According to (Table 4) above the constancy ratio (CR) values of landslide influences are less than 0.1, thus the matrixes satisfy the consistency requirement which is shown in (Tables 2 and 3).

3.5. LSM based on frequency ratio method

According to (Park et al., 2013; Jaafari et al., 2014; Lee et al., 2016) frequency ratio is the ratio of the probabilities of a landslide occurrence to a nonoccurrence for a given attribute (Magliulo et al., 2008). The 8 influencing factors, including slope gradient, slope aspect, land use/-cover, altitude/elevation, road proximity, river proximity, lithology, and rainfalls were employed for the preparation of LSM by the FR model (Table 5).

A higher LSI means higher susceptibility to landslides while a lower LSI indicates a lower susceptibility to landslides (Park et al., 2013; Lee et al., 2004; Ermias, 2014; Colkesen et al., 2016). From the calculated frequency ratio values (Table 5) above can say, that if the ratio is greater than 1, the relationship between landslides and corresponding factors is greater, and if the ratio is less than 1 this means the relationship is less. As stated above in (Equation (5)) the Landslide Susceptibility Index (LSI) is the summation of each factor of frequency ratio value and it can be done/calculated as follows.

LSI = (FR of Slope Degree) + (FR of Slope Aspect) + (FR of Land use/Cover) + (FR of Altitude) + (FR of Distance from Road) + (FR of Distance from River) + (FR of Lithology) + (FR of Precipitation).

According to the landslide susceptibility map produced by the FR model, the total areas of landslide susceptibility zones and landslide falls in this zoned area are *29 %, 32.9 %, 26.1 %, 12 %,* and 7.5%, 28%, 25.9%, 38.6% respectively for low, moderate, high and very high susceptibility (Table. 6.). Landslide susceptibility mapping produced by AHP of the total area is determined by low, moderate-high and very high landslide susceptibility zones making up *0.7 %, 24.3 %, 65.5 %, 9.5 %,* and 0%, 31%, 38.5%, 30.5% for percent area and landslides in this zone respectively (Table 6). It was found that a combination of all these factors which include: slope angle, aspect, lithology, distance road, distance river, precipitation, land use/cover, and altitude contributed to the landslides in the area (Tables 3 and 5).

3.6. Landslide susceptibility maps validation and verification

This was done by overlaying the preexisting landslides (landslide inventories) over the produced landslide susceptibility maps. The best landslide susceptibility map validation methods were selected upon the results of an ROC curve analysis, which was used to obtain success and prediction rates for each scenario (Sinčić et al., 2022; Kalantar et al., 2020; Chowdhuri et al., 2021). The generated maps were validated to cross-check whether the predictions matched or not the expected results (Fig. 13). This was done by overlaying the landslide inventory map with the landslide hazard map and the number of landslides falling in each susceptibility zone was calculated. As can be noted from (Fig. 14) below, most of the recorded active landslides took place in areas that the model has predicted as high landslide susceptibility zones. From the comparison map produced by AHP, 69 % of the active landslide inventory maps fall on high and very high landslide susceptibility zones. Whereas the comparison map produced by FR mode (Fig. 12) shows that 64.5% of active landslide inventory falls on high and very high landslide susceptibility zonation maps (Table 6) and (Fig. 14).

Table: 3
Interior Pair-wise judgment matrixes for sub-class of the causative factors.

Sub Class	[1]	[2]	[3]	[4]	[5]	[6]	[7]	[8]	Weight
Road Proximity									
[1] 0-1000	1	2	3	4	5	8	9		0.360
[2] 1000-2000	1/2	1	2	4	5	6	7		0.258
[3] 2000-3000	1/3	1/2	1	2	3	4	5		0.151
[4] 3000-4000	1/4	1/4	1/2	1	2	3	4		0.097
[5] 4000-5000	1/5	1/5	1/3	1/2	1	2	3		0.064
[6] 5000-6000	1/8	1/6	1/4	1/3	1/2	1	2		0.041
[7] >6000	1/9	1/7	1/5	1/4	1/3	1/2	1		0.028
	[1]	[2]	[3]	[4]					
Lithology									
[1] Limestone	1	2	3	5					0.476
[2] Sandstone	1/2	1	2	4					0.288
[3] Basalts	1/3	1/2	1	2					0.151
[4] Alluvial	1/5	1/4	1/2	1					0.081
	[1]	[2]	[3]	[4]	[5]				
Slope Degree									
[1] >40	1	3	6	7	8				0.514
[2] 30-40	1/3	1	3	4	7				0.250
[3] 20-30	1/6	1/3	1	3	4				0.126
[4] 10 - 20	1/7	1/4	1/3	1	3				0.072
[5] 0-10	1/8	1/7	1/4	1/3	1				0.038
	[1]	[2]	[3]	[4]	[5]	[6]	[7]	[8]	
Slope Aspect									
[1] East	1	1.5	2	3	4	5	6	7	0.292
[2] Northeast	1/1.5	1	1.5	2	3	4	5	6	0.217
[3] Southeast	1/2	1/1.5	1	1.5	2	3	4	5	0.159
[4] South	1/3	1/2	1/1.5	1	1.5	2	3	4	0.113
[5] Southwest	1/4	1/3	1/2	1/1.5	1	2	2	3	0.084
[6] West	1/5	1/4	1/3	1/2	1/2	1	2	3	0.062
[7] Northwest	1/6	1/5	1/4	1/3	1/2	1/2	1	2	0.043
[8] North	1/7	1/6	1/5	1/4	1/3	1/3	1/2	1	0.030
	[1]	[2]	[3]						
Precipitation (mm)									
[1] 2185.02–2292.92	1	2	3						0.525
[2] 2172.07–2185.02	1/2	1	3						0.334
[3] 2115.96–2172.07	1/3	1/3	1						0.142
	[1]	[2]	[3]	[4]	[5]	[6]			
Land use/Cover									
[1] Bare Land	1	2	2	4	5	7			0.354
[2] Water Bodies	1/2	1	2	4	5	6			0.275
[3] Grass Land	1/2	1/2	1	2	3	5			0.172
[4] Cultivated Land	1/4	1/4	1/2	1	2	4			0.101
[5] Shrub Land	1/5	1/5	1/3	1/2	1	2			0.061
[6] Forest Land	1/7	1/6	1/5	1/4	1/2	1			0.037
	[1]	[2]	[3]	[4]	[5]				
Altitude (m)									
[1] 2166-2433	1	2	3	5	6				0.435
[2] 1830-2166	1/2	1	2	3	5				0.265
[3] 1570-1830	1/3	1/2	1	2	3				0.154
[4] 1350-1570	1/5	1/3	1/2	1	2				0.090
[5] 738-1350	1/6	1/5	1/3	1/2	1				0.055
	[1]	[2]	[3]	[4]	[5]	[6]	[7]		
River Proximity (m)									
[1] 0-250	1	2	3	4	5	6	7		0.331
[2] 250-500	1/2	1	3	4	5	6	7		0.268
[3] 500-750	1/3	1/3	1	3	5	5	6		0.178
[4] 750-1000	1/4	1/4	1/3	1	2	3	4		0.092
[5] 1000-1250	1/5	1/5	1/5	1/2	1	2	3		0.056
[6] 1250-1500	1/6	1/6	1/5	1/3	1/2	1	2		0.042
[7] >1500	1/7	1/7	1/6	1/4	1/3	1/2	1		0.029

4. Possible recommendations for mitigation measures

Agricultural activities are a common practice in these areas, and infrastructure (road networks) is important to facilitate and process these agricultural goods, which are largely produced in this area. In the present study, it was found that a combination of different factors was responsible for slope instability. As a result, a combination of different mitigation measures should be used to reduce or eliminate instabilities. According to the findings of the study, the following corrective measures should be implemented in landslide-affected and -prone areas:

Manage steep slope cuts: In the study area, the road cuts are steep slope cuts in almost all parts of the road sections (around Wete, Mededa, the entrance of Gasera gorge, and the Wabe river cuts). The geological materials show a high degree of weathering, are fractured, and are covered by slope-deposited materials. Such areas should be treated with a well-organized and thoroughly researched slope-cutting technique. The poorly graded slope deposits, highly weathered basalts, and road cut deposits become unstable in the steep rock mass cuts. These loose materials, which are dumped down the slope in an unplanned manner, are eroded and slide easily. Therefore, it is necessary to design proper slope cuts along the road corridor and select a planned dumping area for road-cut materials.

Table: 4
The Evaluation of n, λ_{max}, CI, RI, and CR for causative factors.

Causative Factors	n	λ_{max}	CI	RI	CR
All data Layers (Parameters)	8	8.589	0.084	1.41	0.060
Slope Degree	5	5.166	0.041	1.12	0.037
Slope Aspect	8	8.649	0.093	1.41	0.066
Land Use/Cover	6	6.416	0.083	1.24	0.067
Elevation (m)	5	5.331	0.083	1.12	0.063
Road Proximity (m)	7	7.328	0.055	1.32	0.041
River Proximity (m)	7	7.469	0.094	1.32	0.071
Lithology	4	4.183	0.061	0.90	0.068
Precipitation (mm)	3	3.097	0.048	0.58	0.083

Proper management of drainages: During field investigation at different parts of the road corridors or roadsides, it was observed that road parts are eroded and disturbed due to improper management and the lack of drainage systems and culverts. This implies that proper management of culverts and ditches is needed in this area. In general, at the gorge's entrance, particularly at Gasera Parts, the construction of trench drains, culverts, and ditches with water diverted into existing natural or artificial drainage systems is a better solution for roadside erosion and failure.

Supporting **critical slope**s: This technique is recommended for the road section from Gasera town to Wabe River, particularly around the area of Wete and Balo Habebe, starting from the entrance of the gorge at Gasera. It covers a total of 1.5 km for those with severe slope deposits and debris slides. There is also a need for retaining structures to stabilize the rockfalls and rock slides along the road corridors at Wabe River, which are cut on limestone units on the left and right sides of the river

Table. 6
Percentage of landslide susceptibility zones and percentage of active landslide distribution.

Zone	(AHP)		(FR)	
	% Area in pixel	% Landslide area	% Area in pixel	% Landslide area
Low	0.7	0	29.0	7.5
Moderate	24.3	31	32.9	28
High	65.5	38.5	26.1	25.9
V. High	9.5	30.5	12.0	38.6
Total	100	100	100	100

Table. 5
Evaluation of Landslide Causative Factors in Gasera to Indeto Road Landslide affected area, Southeastern Ethiopia.

No	Factors	Subclass	Subclass area % (a)	Landslide in sub-class) % (b)	Ratio (b/a)	Remarks
1	Slope Degree	0–10	20.01	6.71	0.34	
		10–20	20	13.9	0.7	
		20–30	20	15.11	0.76	
		30–45	20	20.61	1.03	
		>45	20	43.67	2.18	
		Total	**100**	**100**	**5**	
2	Slope Aspect	Northeast	16.08	4.94	0.31	
		East	11.85	19.12	1.61	
		Southeast	9.31	20.28	2.18	
		South	15.08	11.29	0.75	
		Southwest	15.27	16.24	1.06	
		West	10.07	23.37	2.32	
		Northwest	8.72	4.77	0.55	
		North	13.63	0	0	
		Total	**100**	**100**	**8.78**	
3	Land use/Cover	Cultivated Land	15.91	0.15	0.01	
		Forest Land	25.06	26.47	1.06	
		Grass Land	52.08	58.12	1.12	
		Shrub Land	4.23	0	0	
		Water Bodies	0.27	0	0	
		Bare Land	2.45	15.26	6.22	
		Total	**100**	**100**	**8.41**	
4	Altitude (m)	738–1350	20.05	34.16	1.7	
		1350–1570	20.03	8.62	0.43	
		1570–1830	19.97	8.76	0.44	
		1830–2166	19.98	47.51	2.38	
		2166–2433	19.96	0.94	0.05	
		Total	**100**	**100**	**5**	
5	Road Proximity (m)	0–1000	17.27	31.08	1.8	
		1000–2000	15.9	6.78	0.43	
		2000–3000	15.74	15.06	0.96	
		>3000	14.86	18.68	1.26	
		Total	**100**	**100**	**6.95**	
6	River Proximity (m)	0–500	31.97	44.52	1.39	
		500–1000	23.69	27.79	1.17	
		1000–1500	16.63	17.75	1.07	
		>2000	10.74	6.31	0.59	
		Total	**100**	**100**	**5.03**	
7	Lithology	Alluvial	15.34	1.14	0.07	
		Basalts	49.18	65.21	1.33	
		Sandstone	23.81	1.74	0.07	
		Limestone	11.67	31.9	2.73	
		Total	**100**	**100**	**4.21**	
8	Precipitation (mm)	2115.96–2172.07	16.63	14.47	0.87	
		2172.07–2185.02	50.59	70.52	1.39	
		2185.02–2292.92	32.78	15.01	0.46	
		Total	**100**	**100**	**2.72**	

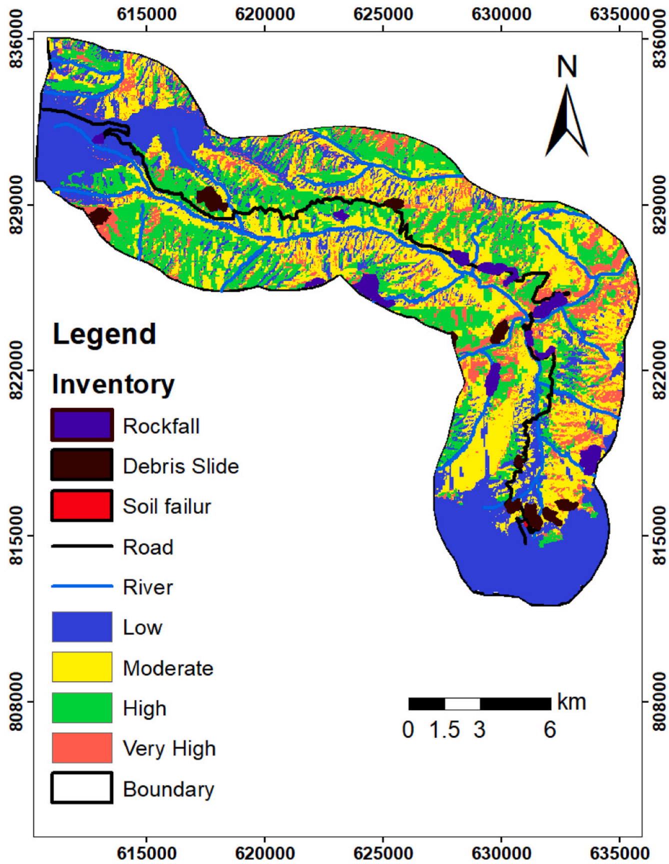

Fig. 12. Landslide susceptibility map produced by Frequency ratio model.

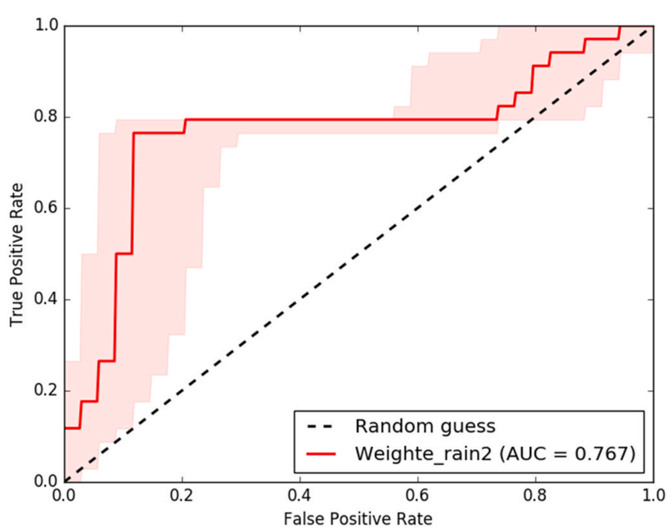

Fig. 13. Shows the area under the curve (AUC) map for validation.

(Fig. 5 a). In the study area around the Wondecho River, a retaining wall is not fully functional and is affected by debris slides. Therefore, the retaining structures that will be constructed should be properly designed in such a way that they resist the load imposed by the slide material and have sufficient drainage outlets.

Creating awareness: People who live in Wete, Hora, Meddeda, Balo Habibe, and Werdubey do so because of the fertile soil, availability of various streams, and proximity to Gasera town. So, it is very important to provide awareness-building education for these localities. Generally, from the fi–eld observations, in some places, the sloppy areas were used for house construction and agricultural activities. Therefore, it is very important to create awareness among the residents to minimize the adverse effects of mismanaged man-made activities. Local people should take care of the landslides that happened previously in their surroundings, and instead of deforestation, they should develop afforestation practices on slopes to improve the stability of slopes to a certain degree.

Resettlement: According to the landslide susceptibility mapping of the study area during the present study, the slopes that fall in high and very high hazard zones are susceptible to future landslide activities. Even the validation of the landslide susceptibility map revealed that all past landslide activities fell within high and very high-hazard zones. Thus, such high and very high hazard zones should be avoided for any settlements, and those who are in them must be rehabilitated to a safer area. The Gasera Gorge, Wete, and Hora areas, which have a large number of settlements and are highly vulnerable to and affected by active landslides, as well as the Werdubey Wabe river cut areas, where people are settled following the Wabe river and using river-deposited materials for agricultural activity, should be resettled and/or made aware of the problem.

Afforestation practice and minimize deforestation: Around Wete, Mededa, Tsebela, Balo, and Hora, parts of the study area are covered by slope-deposited and highly weathered basaltic materials that are used for agricultural fields due to their fertility and shortage of farmlands. In this area, some trees and bushes are removed to make way for more agricultural fields. So, these areas should stop deforestation and develop afforestation. This may increase the stability of some unstable slope areas.

5. Discussion

Geohazard Mapping and Mitigation along the Road Gasera–Indeto, Oromia Regional State, and Southeast Ethiopia were done using GIS-based AHP and FR methods. The results of the study show that the LSM produced by AHP methods was 69% correlated with the existing landslides as produced inventory during the field investigations. Whereas the LSM produced using FR techniques showed and or correlated 64.5% with the existing landslides in the field in general.

The study found that among the selected causative factors, the lithology, slope, and aspect based on their contributing orders were the main contributing factors contributing to slope instability in the study area. Based on the detailed investigations among the selected causative factors for this study, Lithology shows the highest contributions to the occurrence of landslides in the area. The basaltic and Limestone formations are identified by this study due to their nature of fragile, the geological units in the area, especially in limestone, sandstone, and basalt units, can aggravate the instability of slopes.

Among the basaltic units, the doleritic intrusions are the leading ones to contribute to the sliding hazards in the area this is due to the spheroidal nature and weathering of the hosting materials this means during the rainy season the hosting materials surrounding the dolerites that are used as cement are washed out and following this mass of sliding have occurred in this unit. The Aphanitic intercalated with scoria basalt also shows a weakness in between the intercalated joints due to the weathering nature that allows water to flow through it the finally the units detached from each other.

Lithological boundaries and jointed rocks when they become weathered lose their cementation nature of boundary and joints finally huge blocks of rocks are detached from the area as rockfalls (Fig. 5a–and Fig. 10). The sedimentary terrains also the area suspected to the driving factor for the occurrences of the landslides in the area in the limestone unit because of the lithological boundaries and joints occurred between the limestone marl intercalations. As can be seen from the meteorological data that is recorded from four stations in the study area, the area receives an average of 2000 m3/year of rain. This implies that due to the fragile nature of the geological units in the area, especially in limestone, sandstone, and basalt units, can aggravate the instability of slopes.

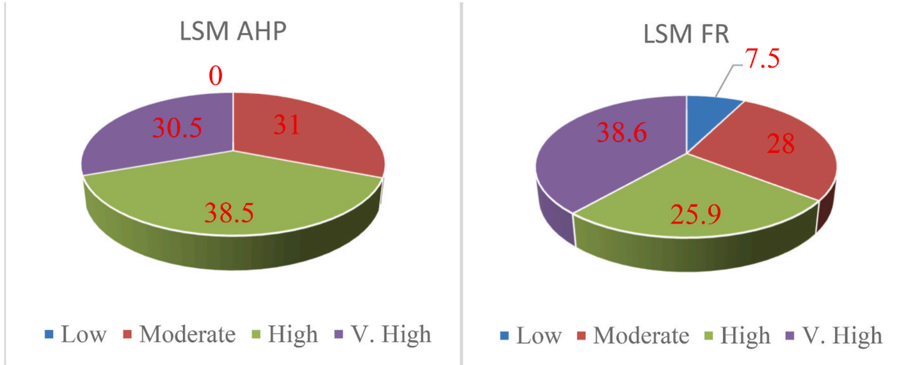

Fig. 14. Chart showing the relationship between area coverage and percent of active landslides.

In this study, a GIS-based analytical hierarchy process and frequency ratio model using eight landslide causative factors have been analyzed, and the resulting map has been classified into four zones of low, moderate, high, and very high classes. According to the landslide susceptibility maps and field observations, road corridors have the highest frequency of landslides. This is because of the steepening of the road-cut slope, the weight of slope deposits during the rainy season, and road-cut dumps, all of which contribute to unstable underlying support materials.

6. Conclusions

The study was carried out to map the landslide susceptibility of the road corridor and the surrounding areas of the Gaser to Indeto road with buffer zones of 10 km from the road. The study followed GIS-based AHP and FR methods with the combinations of eight selected landslide conditioning factors called slope, aspect, lithology, rainfall, altitude, road proximity, river proximity, and land use/cover. The result of the study shows that 64.5 % and 69 % of LSM produced by FR and approaches respectively show the highest landslide occurrences in the area and are highly correlated with the inventory map produced during the field study. The landslide hazard zonation mapping resulting based on the analytical hierarchy process of the total study area showed that 0%, 31%, 38.5 %, and 30.5% of low, moderate, high, and very high respectively are vulnerable to landslides. Whereas the landslide hazard zonation map based on the Frequency ratio approach showed that 7.5%, 28%, 25.9%, and 38.6% of low, moderate, high, and very high respectively are vulnerable to landslides.

In general, it was found that a combination of all these factors which include: slope angle, aspect, lithology, distance road, distance river, precipitation, land use/cover, and altitude contributed to the occurrence of landslides in the area directly and indirectly. The fragile nature of the geology, the very steepness of the sloppy area, and the aspects of the daylighting all together as integration bring the landslides in the wabe Shebelle Gorge area.

Slope instability in the study area is manifested in the form of soil failure and debris flow, and at some places, rockfalls are commonly observed. The debris flows were composed of soil, rock fragments of varied sizes, vegetation, and plant roots. From field observations, it has been found that most of the slope instability is induced by the combination of several factors; therefore, an integrated approach of remedial measures may help minimize landslide hazards in the area. However, more detailed studies would be required to work out specific remedial measures for individual critical slope sections. The produced landslide susceptibility map is very important for urban planners, agricultural studies, environmentalists, and future landslide hazardous prevention and mitigation strategies of the area.

Funding source

There is no external funding source for this research work.

Declaration of competing interest

I am delighted to submit the manuscript, *Geohazard Mapping and Mitigations along Road the Gasera–Indeto, Southeast Ethiopia*, of the original research paper for publication. I believe these findings will be of interest to the readers of your journal. I declare that this manuscript is original, has not been published before, and is not currently being considered for publication elsewhere. I declare that no conflicts of interest are associated with this publication, and there has been no significant financial support for this work that could have influenced its outcome.

Acknowledgments

I thank you the editors and the anonymous reviewers of this journal.

Data availability

Data will be made available on request.

References

Ahmad, M.S., Khan, S., 2023. Comparative analysis of analytical hierarchy process (AHP) and frequency ratio (FR) models for landslide susceptibility mapping in Reshun, NW Pakistan. Kuwait Journal of Science 50 (3), 387–398.
Anbalagan, R., Kumar, R., Lakshmanan, K., Parida, S., Neethu, S., 2015. Landslide hazard zonation mapping using frequency ratio and fuzzy logic approach, a case study of Lachung Valley, Sikkim. Geoenvironmental Disasters 2 (1), 1–17.
Asmare, D., 2022. Landslide hazard zonation and evaluation around Debre Markos town, NW Ethiopia—a GIS-based bivariate statistical approach. Scientific African 15, e01129.
Asmare, D., Tesfa, C., 2022. Application and validation of the evaluation using slope stability susceptibility evaluation parameter rating system to debre werk area (Northwest Ethiopia). Geotech. Geol. Eng. 40 (5), 2475–2488.
Asmare, D., Tesfa, C., Zewdie, M.M., 2023. A GIS-based landslide susceptibility assessment and mapping around the Aba Libanos area, Northwestern Ethiopia. Applied Geomatics 15 (1), 265–280.
Choudhury, D., Das, T., Rao, V.D., 2024. Case studies and numerical investigation of landslide triggering mechanisms in Western Ghats, Kerala, India. Indian Geotech. J. 54 (1), 96–108.
Chowdhuri, I., Pal, S.C., Chakrabortty, R., Malik, S., Das, B., Roy, P., et al., 2021. Spatial prediction of landslide susceptibility using projected storm rainfall and land use in Himalayan region. Bull. Eng. Geol. Environ. 80 (7), 5237–5258.
Colkesen, I., Sahin, E.K., Kavzoglu, T., 2016. Susceptibility mapping of shallow landslides using kernel-based Gaussian process, support vector machines and logistic regression. J. Afr. Earth Sci. 118, 53–64.
Das, T., Rao, V.D., Choudhury, D., 2022. Numerical investigation of the stability of landslide-affected slopes in Kerala, India, under extreme rainfall event. Nat. Hazards 114 (1), 751–785.
Dastranj, A., Noor, H., 2021. Comparative evaluation of landslide susceptibility map using Analytical Hierarchy Process (AHP) and Fuzzy methods. Journal of RS and GIS for Natural Resources 12 (3), 62–81.

Desalegn, H., Mulu, A., Damtew, B., 2022. Landslide susceptibility evaluation in the Chemoga watershed, upper Blue Nile, Ethiopia. Nat. Hazards 1–27.

Dos Santos, P.H., Neves, S.M., Sant'Anna, D.O., de Oliveira, C.H., Carvalho, H.D., 2019. The analytic hierarchy process supporting decision making for sustainable development: an overview of applications. J. Clean. Prod. 212, 119–138.

Ermias, B., 2014. Landslide Hazard Zonation Around the Route from Alemketema Town to Ambat Village. Addis Ababa University, North Shewa, Ethiopia.

Gnyawali, K.R., Shrestha, R., Bhattarai, A., Magar, P.R., Dhungana, A.R., Sukupayo, I., et al., 2015. Rockfall characterization and structural protection in the siddhababa section of siddhartha highway H10, Nepal. J. Inst. Eng. 11 (1), 1–11.

Hamza, T., Raghuvanshi, T.K., 2017. GIS based landslide hazard evaluation and zonation–A case from Jeldu District, Central Ethiopia. J. King Saud Univ. Sci. 29 (2), 151–165.

Haque, U., Da Silva, P.F., Devoli, G., Pilz, J., Zhao, B., Khaloua, A., et al., 2019. The human cost of global warming: deadly landslides and their triggers (1995–2014). Sci. Total Environ. 682, 673–684.

Hewitt, K., 2016. The human ecology of disaster risk in cold mountainous regions. Oxford Research Encyclopedia of Natural Hazard Science.

Jaafari, A., Najafi, A., Pourghasemi, H., Rezaeian, J., Sattarian, A., 2014. GIS-based frequency ratio and index of entropy models for landslide susceptibility assessment in the Caspian forest, northern Iran. Int. J. Environ. Sci. Technol. 11 (4), 909–926.

Kalantar, B., Ueda, N., Saeidi, V., Ahmadi, K., Halin, A.A., Shabani, F., 2020. Landslide susceptibility mapping: machine and ensemble learning based on remote sensing big data. Rem. Sens. 12 (11), 1737.

Landslide hazard zonation mapping using frequency ratio and fuzzy logic approach, A case study national road n° 11 (Bizerte-Béja: northern Tunisia). In: Klai, A., Bouzid, M.K., Haddad, R., Rabia, M.C. (Eds.), 2017. Euro-Mediterranean Conference for Environmental Integration. Springer.

Korup, O., Stolle, A., 2014. Landslide prediction from machine learning. Geol. Today 30 (1), 26–33.

Lee, S., Talib, J.A., 2005. Probabilistic landslide susceptibility and factor effect analysis. Environmental Geology 47 (7), 982–990.

Lee, S., Ryu, J.-H., Won, J.-S., Park, H.-J., 2004. Determination and application of the weights for landslide susceptibility mapping using an artificial neural network. Eng. Geol. 71 (3–4), 289–302.

Lee, M., Park, I., Won, J., Lee, S., 2016. Landslide hazard mapping considering rainfall probability in Inje, Korea. Geomatics, Nat. Hazards Risk 7 (1), 424–446.

Lin, Q., Steger, S., Pittore, M., Zhang, J., Wang, L., Jiang, T., et al., 2022. Evaluation of potential changes in landslide susceptibility and landslide occurrence frequency in China under climate change. Sci. Total Environ. 850, 158049.

Magliulo, P., Di Lisio, A., Russo, F., Zelano, A., 2008. Geomorphology and landslide susceptibility assessment using GIS and bivariate statistics: a case study in southern Italy. Nat. Hazards 47 (3), 411–435.

Millet, I., Saaty, T.L., 2000. On the relativity of relative measures–accommodating both rank preservation and rank reversals in the AHP. Eur. J. Oper. Res. 121 (1), 205–212.

Mishra, V., Malik, K., Agarwal, V., Mishra, P.K., Jain, K., 2024. Impact assessment of unsustainable airport development in the Himalayas using remote sensing: a case study of Pakyong Airport, Sikkim, India. Quaternary Science Advances 13, 100144.

Park, S., Choi, C., Kim, B., Kim, J., 2013. Landslide susceptibility mapping using frequency ratio, analytic hierarchy process, logistic regression, and artificial neural network methods at the Inje area, Korea. Environ. Earth Sci. 68 (5), 1443–1464.

Saaty, T.L., 2008. Decision making with the analytic hierarchy process. Int. J. Serv. Sci. 1 (1), 83–98.

Sinčić, M., Bernat Gazibara, S., Krkač, M., Mihalić Arbanas, S., 2022. Landslide susceptibility assessment of the City of Karlovac using the bivariate statistical analysis. Rudarsko-Geolosko-Naftni Zb. 38 (2), 149–170.

Soni AK, Rawat R, Jain V, Panday SK. Landslide Susceptibility Mapping along Mumbai-Pune Expressway, Western Ghats, Maharashtra Using Remote Sensing and GIS. 2022.

Tesfa, C., 2022. GIS-based AHP and FR methods for landslide susceptibility mapping in the abay gorge, dejen–renaissance bridge, central, Ethiopia. Geotech. Geol. Eng. 1–15.

Tesfa, C., Sewnet, D., 2024. GIS-based MCDM approach for landslide hazard zonation mapping in east gojjam zone, Central Ethiopia. Quaternary Science Advances, 100210.

Tesfa, C., Woldearegay, K., 2021. Characteristics and susceptibility zonation of landslides in Wabe Shebelle Gorge, south eastern Ethiopia. J. Afr. Earth Sci. 182, 104275.

Voogd, H., 1988. Multicriteria evaluation: measures, manipulation, and meaning—a reply. Environ. Plann. Plann. Des. 15 (1), 65–72.

Wang, Q., Li, W., 2017. A GIS-based comparative evaluation of analytical hierarchy process and frequency ratio models for landslide susceptibility mapping. Phys. Geogr. 38 (4), 318–337.

Wicki, A., Lehmann, P., Hauck, C., Stähli, M., 2022. Impact of topography on in-situ soil wetness measurements for regional landslide early warning–a case study from the Swiss Alpine Foreland. Natural Hazards and Earth System Sciences Discussions 1–28.

Woldearegay, K., 2013. Review of the occurrences and influencing factors of landslides in the highlands of Ethiopia: with implications for infrastructural development. Momona Ethiopian Journal of Science 5 (1), 3–31.

Wyllie, D.C., Mah, C., 2004. Rock Slope Engineering. CRC Press.

Zhu, Z., Gan, S., Yuan, X., Zhang, J., 2022. Landslide susceptibility mapping with integrated SBAS-InSAR technique: a case study of Dongchuan District, Yunnan (China). Sensors 22 (15), 5587.